Cell. Mol. Life Sci. 63 (2006) 0112–0121
1420-682X/06/010112-10
DOI 10.1007/s00018-005-5303-0
© Birkhäuser Verlag, Basel, 2006

Cellular and Molecular Life Sciences

Research Article

Activation of the human FP prostanoid receptor disrupts mitosis progression and generates aneuploidy and polyploidy

X.-B. Chen and J. W. Regan*

Department of Pharmacology & Toxicology, College of Pharmacy, The University of Arizona, Tucson, Arizona 85721-0207 (USA), Fax: +1 520 626 2466, e-mail: regan@pharmacy.arizona.edu

Received 7 July 2005; received after revision 22 October 2005; accepted 11 November 2005
Online First 27 December 2005

Abstract. Studies have shown prostaglandin $F_{2\alpha}$ ($PGF_{2\alpha}$) to be an endogenous tumor promoter in mouse models of skin carcinogenesis; however, the mechanisms by which $PGF_{2\alpha}$ affects cell cycle events remain unknown. Here we performed cell cycle analyses on HEK cells stably expressing the human FP receptor and found that treatment with $PGF_{2\alpha}$ delays mitosis and is associated with an increased expression of cyclin B1 and Cdc2 kinase activity. In addition, multipolar spindles and misaligned chromosomes were observed in a significant proportion of cells treated with $PGF_{2\alpha}$. Defective cytokinesis was also observed which resulted in gross aneuploidy and polyploidy. Expression of dominant negative Rho attenuated the cell cycle delay and prevented the generation of micronuclei following treatment with $PGF_{2\alpha}$. This suggests that FP receptor activation of Rho signaling by $PGF_{2\alpha}$ can interfere with nuclear division. Aneuploidy is associated with genomic instability and may underlie the tumor-promoting properties of $PGF_{2\alpha}$.

Key words. FP prostanoid receptor; cell cycle; cyclin B1; Cdc2; RhoA; cytokinesis; aneuploidy; polyploidy.

Prostaglandin $F_{2\alpha}$ ($PGF_{2\alpha}$) belongs to the family of prostanoids that are derived from arachidonic acid by the sequential actions of the cyclooxygenases (COXs) and the respective prostaglandin (PG) and thromboxane (Tx) synthases. Prostanoids, which include PGE_2, $PGF_{2\alpha}$, PGI_2, PGD_2, and TxA_2, are synthesized in nearly all human tissues and act in an autocrine/paracrine manner to elicit a broad spectrum of physiological and pathophysiological actions. Some of these actions include inflammation, wound healing, kidney function, bone metabolism, immune response, and reproductive function [1]. In the context of pathological conditions, specifically in tumors, a large body of evidence from epidemiological, *in vivo,* and *in vitro* studies suggests the involvement of COX-2 and its downstream effectors PGE_2 and $PGF_{2\alpha}$ in multistage carcinogenesis, particularly in tumor promotion [2, 3]. More recent studies using transgenic mice have suggested a direct prooncogenic role for COX-2 and have shown that targeted overexpression of COX-2 is sufficient to induce hyperplasia, dysplasia, and tumorigenesis [4, 5]. Furthermore, PGE_2 has been found to participate in tumorigenesis by inhibiting apoptosis, promoting cell proliferation and survival, and by inducing angiogenesis and immunosuppression [6–8]. Positive feedback between COX-2 and PGE_2 has also been suggested to facilitate malignant transformation [9]. Compared to PGE_2, there is less information available on the molecular mechanisms involved in the tumor-promoting activity of $PGF_{2\alpha}$.

$PGF_{2\alpha}$ binds to what has been defined as the FP prostanoid receptor, which belongs to the family of heterotrimeric G protein-coupled receptors (GPCRs) [10]. The FP prostanoid receptor is coupled to Gq, and stimulation of the receptor by $PGF_{2\alpha}$ leads to the activation of phospholipase C-β (PLCβ) signaling followed by downstream activation of protein kinase C (PKC) and an elevation in intracellu-

* Corresponding author.

lar Ca^{2+} [10, 11]. The $PGF_{2\alpha}$-induced activation of PKC has been demonstrated to activate the Raf/MEK/MAP kinase signaling cascade and to stimulate cell proliferation [12, 13]. In addition, activation of MAP kinase by $PGF_{2\alpha}$ can be inhibited by pertussis toxin, suggesting that FP receptor can also couple to G_i [14]. Recent studies using HEK 293 cells stably expressing alternative mRNA splice variants of the ovine FP receptor demonstrated that $PGF_{2\alpha}$ could stimulate the activation of Rho GTPase signaling leading to actin-mediated changes in cell morphology and activation of focal adhesion kinase [15].

The growth of cells in a tissue essentially represents a balance between cellular death or apoptosis, and cellular proliferation. Growth will occur if apoptosis decreases and proliferation increases, or a combination thereof. Cellular proliferation reflects the activity of the cell cycle, which is driven by the interaction of cyclins with the cyclin-dependent kinases (CDKs) [16]. Different cyclin-CDK complexes are activated at different points in the cell cycle. The transition of cells from G2 to mitosis is dependent upon the completion of several events that culminate in the activation of the cyclin B/Cdc2 kinase complex [17].

During mitosis, cells undergo nuclear division in which the duplicated chromosomes are partitioned equally between the two daughter cells. The mitotic spindle plays an essential role in this complex movement, which depends on the proper assembly, orientation and attachment of the spindle to the chromosomes. Missegregation of the duplicated chromosomes can result from abnormal spindles and/or misalignment of the chromosomes and can give rise to the gain or loss of chromosomes (aneuploidy). Genomic instability is a hallmark of tumorigenesis and the development of polyploidy and aneuploidy is one established mechanism for generating genomic instability during tumorigenesis.

Using the mouse skin model of multistage carcinogenesis, $PGF_{2\alpha}$ has been identified as an endogenous tumor promoter [18, 19]. The exact mechanisms by which $PGF_{2\alpha}$ promotes skin tumorigenesis are unknown but could involve increased cell proliferation, decreased apoptosis or immune surveillance, or combinations of these processes. Studies have shown that $PGF_{2\alpha}$ can stimulate cellular proliferation, although not specifically in the context of skin tumorigenesis [20, 21]. In the present study we performed a detailed cell cycle analysis on HEK cells stably expressing the human FP receptor. Activation of the FP receptor by $PGF_{2\alpha}$ was found to disrupt mitosis progression, generating abnormal mitotic spindles and misaligned chromosomes. In addition, prolonged stimulation with $PGF_{2\alpha}$ lead to the development of polyploidy and aneuploidy. Expression of dominant negative Rho attenuated the changes in cell cycle progression and rescued the aneuploidy caused by $PGF_{2\alpha}$ treatment. These findings show that $PGF_{2\alpha}$-induced Rho signaling interferes with nuclear division and suggest that the tumor-promoting activity of $PGF_{2\alpha}$ could be a consequence of resulting genomic instability.

Materials and methods

Reagents. Dulbecco's modified Eagle's medium (DMEM), Opti-MEM, fetal bovine serum (FBS), G418, gentamicin, and hygromycin B were purchased from Life Technologies. [γ-^{32}P]ATP was purchased from Amersham Biosciences. $PGF_{2\alpha}$ was purchased from Cayman Chemicals. Bromodeoxyuridine (BrdU) and propidium iodide, and anti-a-tubulin monoclonal antibody were purchased from Sigma and prepared in phosphate-buffered saline (PBS) as 1 mM and 1 mg/ml stock solutions, respectively. Anti-α-tubulin monoclonal antibody was purchased from Sigma. Monoclonal anti-cyclin B1 and anti-BrdU antibodies were purchased from BD Transduction Laboratories. Cdc2 rabbit polyclonal (C-19) and mouse monoclonal (B-6) antibodies were purchased from Santa Cruz Biotechnology. Histone H1 and monoclonal anti-actin antibodies were purchased from Calbiochem. Texas red isothiocyanate-conjugated phalloidin, Alexa Fluor 488-, and Alexa Fluor 594-conjugated anti-mouse secondary antibodies were purchased from Molecular Probes. Horseradish peroxidase (HRP)-conjugated anti-mouse secondary antibody was purchased from Promega. The FuGENE 6 transfection kit was purchased from Roche. Protein G-Sepharose was purchased from Amersham Biosciences.

Cell culture and transient transfections. HEK 293 EBNA cells (Invitrogen) stably expressing the human FP receptor (hFP-HEK) and empty vector (pCEP4)-transfected cells (pCEP4-HEK) were maintained in DMEM supplemented with 10% FBS, 250 µg/ml G418, 100 µg/ml gentamicin, and 200 µg/ml hygromicin B. Hygromicin B is the selection drug for pCEP4-containing cells. Transient transfections using the FuGENE 6 kit were performed according to the manufacturer's manual. Briefly, cells were split into 35-mm dishes or six-well plates and incubated at 37 °C overnight. Before transfection, 6 µl of FuGENE 6 reagent was incubated with 100 µl of Opti-MEM for 5 min at room temperature and then 2 µg of plasmid DNA was added consisting of one plasmid encoding enhanced green fluorescent protein (EGFP) and a second encoding N19RhoA (used at a ratio of 1:3). After 30 min at room temperature, the FuGENE/DNA solution was added dropwise to the cells and swirled gently, after which the cells were incubated at 37 °C for 24 h and were then used for either cell cycle analysis or immunofluorescence staining.

Synchronization. A thymidine-mimosine double-block protocol was used to synchronize cells in late G1 phase. Cells were plated at a density of ~5×10^5 in 10-cm dishes

and incubated at 37 °C overnight. Cells were then treated with thymidine (2.5 mM; Sigma) for 16 h, after which thymidine was washed away. Eight hours later, mimosine (400 µM; Calbiochem) was added to the cultures for another 16 h. This protocol results in synchronization of more than 90% of cells in the late G1 phase.

BrdU incorporation and cell cycle analysis. Cell cycle analysis was investigated using anti-BrdU/propidium iodide double staining. For each experiment, cells were plated at a density of ~5×10^5 in 10 cm-dishes and incubated at 37 °C for 24 h to permit adherence. Cells were then treated with either vehicle (2% sodium bicarbonate) or 1 µM $PGF_{2\alpha}$ and 24 and 48 h later the cells were pulsed by the addition of 10 µM BrdU to the medium for 10 min at 37 °C. The cells were trypsinized, washed with 1% bovine serum albumin (BSA) in PBS and resuspended in 200 µl ice-cold PBS. Fixation was performed by adding cells dropwise into 5 ml of cold 70% ethanol (glass test tubes) while vortexing and were incubated on ice for an additional 30 min. Cells were then treated at room temperature for 30 min with 2 M HCl containing 0.5% Triton X-100 to denature DNA and neutralized by washing once with 0.1 M borax, pH 8.5. Indirect immunofluorescence was performed by incubating the cells at room temperature for 1 h (or 4 °C overnight) with anti-BrdU monoclonal antibody (1:100) diluted in PBS containing 0.5% Tween and 1% BSA, followed by incubation at room temperature for 1 h with FITC-labeled anti-mouse IgG (1:500) at room temperature for 1 h. The cells were washed once with PBS and resuspended in 0.5 ml of PBS containing 5 µg/ml of propidium iodide and analyzed using a FACScan flow cytometer (Arizona Cancer Center core facilities). The percentage of cells in G1/G0, S, and G2/M were determined using the CellQuest program (BD Biosciences). For cell cycle analysis of EGFP- and N19Rho-transfected cells, cells were prefixed in 1% formaldehyde in PBS on ice for 1 h and then fixed in 70% ethanol at 4 °C overnight. After one wash with PBS, cells were incubated for 30 min in 50 µg/ml propidium iodide solution containing 100 µg/ml RNase A. CellQuest and Modfit programs were used to select cells containing EGFP and to determine cell cycle distribution, respectively.

Immunoblotting. Cells were plated at a density of ~1×10^6 in 10 cm dishes and 24 h later 1 µM $PGF_{2\alpha}$ was added and the cells were incubated for another 24 h at 37 °C. Cell lysates were prepared and immunoblotting was performed as follows. Cells were washed twice with cold PBS and lysed on ice in 500 µl RIPA buffer consisting of 150 mM NaCl, 50 mM Tris-HCl (pH 8.0), 5 mM EDTA, 1% NP-40, 0.5% sodium deoxycholate, 10 mM sodium fluoride, 10 mM disodium pyrophosphate, 0.1% SDS, 1 mM PMSF, 1 mM sodium orthovanadate, 10 µg/ml leupeptin, and 10 µg/ml aprotinin. The samples were rotated at 4 °C for 30 min and centrifuged at 14,000 g for 10 min. The supernatants were measured for protein concentrations (Bradford assay) and 40 µg of protein was loaded on 10% SDS-PAGE gels, electrophoresed, and transferred to nitrocellulose membranes. The membranes were incubated at room temperature for 1 h with blocking buffer consisting of 5% BSA and 0.1% Tween 20 in TBS, followed by an overnight incubation with monoclonal anti-cyclin B1 or monoclonal anti-Cdc2 antibodies (diluted 1:1000 with blocking buffer). HRP-conjugated anti-mouse secondary antibody was used at a dilution of 1:10,000. Immunoreactivity was detected by SuperSignal enhanced chemiluminescence (Pierce). To ensure equal loading of protein, the membranes were reprobed as above after stripping the membranes for 30 min at 55 °C in a stripping buffer consisting of 2% SDS, 62.5 mM Tris (pH 7.6), and 100 mM β-mercaptoethanol.

In vitro Cdc2 kinase assay. The Cdc2 kinase assay was performed according to published procedures as follows [22]. Cells were washed once in ice-cold PBS and incubated for 30 min on ice in a lysis buffer consisting of 50 mM Tris-HCl (pH 7.4), 0.5% NP-40, 150 mM NaCl, 50 mM NaF, 1 mM sodium orthovanadate, 1 mM PMSF, 10 µg/ml leupeptin, and 10 µg/ml aprotinin. The samples were centrifuged at 12,000 rpm for 10 min and 500 µg of protein from the supernatant was immunoprecipitated for 3 h at 4 °C with 2 µg of polyclonal C-19 anti-Cdc2 antibody, and 20 µl of protein G-Sepharose beads (50% w/v). The beads were washed four times in lysis buffer and twice in buffer consisting of 50 mM HEPES (pH 7.4), 10 mM $MgCl_2$, and 1 mM dithiothreitol. The samples were equally divided and one set was used for immunoblotting with anti-Cdc2 monoclonal antibody and the second set was used for the kinase assay. The assay was carried out for 30 min at room temperature in 20 µl of kinase buffer consisting of 50 mM HEPES (pH 7.4), 10 mM $MgCl_2$, 5 µM ATP, 1 mM dithiothreitol, 5 µg histone H1, and 10 µCi [γ-^{32}P]ATP (3000 Ci/mmol). The assay was terminated by adding 5 µl of 5× sample loading buffer and boiled for 5 min at 95 °C. The samples were fractionated by SDS-PAGE, dried, and subjected to autoradiography to visualize the incorporation of ^{32}P into histone H1.

Immunofluorescence microscopy. Immunofluorescence microscopy was performed using an Olympus IX70 microscope and ×60 oil immersion and ×20 objectives. Images were acquired using an Olympus Digital camera and MagnaFire 2.1 acquisition software, and were processed using Adobe Photoshop software. For antibody staining, transfected and non-transfected cells were seeded on poly-lysine-treated coverslips in six-well plates. After treatment with $PGF_{2\alpha}$ for the indicated times, cells were washed once in PBS and fixed for 15 min in 4%

paraformaldehyde in PBS (freshly prepared). The cells were then rinsed three times in 0.1 M glycine (pH 7.4) and permeabilized for 10 min in 2×SSC (30 mM NaCl, 300 mM sodium citrate) containing 0.1% Triton X-100. The cells were washed 3 additional times in PBS and then incubated for 30 min in blocking buffer consisting of 2×SSC, 0.05% Triton X-100, 2% goat serum, 1% BSA followed by a 1-h incubation at room temperature in blocking buffer containing a 1:1000 dilution of Texas red isothiocyanate-conjugated with phalloidin. After a brief wash in PBS, cells were stained with 4, 6-diamidino-2-phenylindole (DAPI) (1 µg/ml) for 10 min and washed three times in PBS and once in water. Coverslips were mounted using p-phenylenediamine. For α-tubulin staining, cells were prefixed in a solution containing 4% formaldehyde, 100 mM HEPES (pH 6.8), 5 mM EGTA, 10 mM $MgCl_2$, and 0.2% Triton X-100 for 10 min at room temperature and then fixed in cold methanol for 10 min at –20 °C. After several washes in PBS, the cells were blocked with 2% BSA in TBST for 30 min at room temperature and then incubated for 1 h with monoclonal anti-α-tubulin antibodies (1:1000 in blocking buffer), followed by a 1-h incubation with Alexa Fluor 488-conjugated secondary antibodies (1:1000 dilution in blocking buffer).

Results

$PGF_{2\alpha}$ treatment of HEK cells expressing the human FP receptor leads to cell cycle delay in G2/M. Flow cytometry was used to investigate the effect of $PGF_{2\alpha}$ on cell cycle progression of HEK cells expressing the human FP prostanoid receptor. Empty vector pCEP4-transfected cells were used as the control. Asynchronous cultures were treated with either 1 µM $PGF_{2\alpha}$ or vehicle for 24 or 48 h and were pulse labeled with 10 µM BrdU for 15 min to mark the S phase of cells undergoing DNA replication. Additionally, the cells were stained with propidium iodide to determine the nuclear DNA content. As shown in figure 1, both vehicle-treated and $PGF_{2\alpha}$-treated pCEP4-HEK cells and vehicle-treated hFP-HEK cells showed similar cell cycle distribution profiles. In contrast, in $PGF_{2\alpha}$-treated hFP-HEK cells, the G1 population was reduced to 30% in the treated cells (compared to 42% in the untreated cells), while there was a corresponding increase in the G2/M population from 12% to 24.5%. These changes were evident after both 24 and 48 h of treatment with $PGF_{2\alpha}$. The S phase population remained relatively constant. The constant S phase population and the similar profile of S phase distribution before and after treatment indicates that $PGF_{2\alpha}$ had no detectable effects on DNA replication as measured by BrdU incorporation. The increase in G2/M population, on the other hand, suggests either a delay in the G2/M transition or in the exit from mitosis.

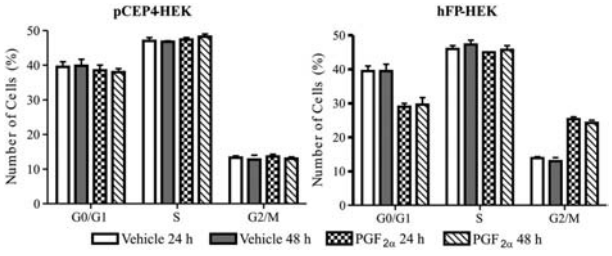

Figure 1. $PGF_{2\alpha}$ increases the G2/M population in HEK cells stably expressing the human FP prostanoid receptor. Histograms of cell cycle distributions of HEK cells stably transfected with either the human FP prostanoid receptor (hFP-HEK) or with the empty vector (pCEP4-HEK) and treated with either vehicle (2% Na_2CO_3) or 1 µM $PGF_{2\alpha}$ for 24 or 48 h. BrdU incorporation, propidium iodine labeling, and two-dimensional flow cytometry were carried out as described in Materials and methods. Data are expressed as a percentage of the number of cells in each phase of the cell cycle and represent the means ± SEs from four independent experiments.

To better understand the effect of $PGF_{2\alpha}$ on the cell cycle, cells were synchronized in late G1 by a double thymidine-mimosine block and then $PGF_{2\alpha}$ or vehicle was added at the time of release from the block. As shown in figure 2, at the time of release (0 h), more than 90% of vehicle-treated pCEP4-HEK cells were in G1; after 6 h, they progressed into S phase and by 9 h a small fraction of cells had exited mitosis. After 15 and 18 h only a negligible G2/M peak remained, as the majority of the vehicle-treated pCEP4-HEK cells had exited mitosis and accumulated in G0/G1. $PGF_{2\alpha}$-treated pCEP4-HEK cells and vehicle-treated hFP-HEK cells showed profiles of cell cycle progression that were very similar to the vehicle-treated pCEP4-HEK cells. In contrast, $PGF_{2\alpha}$ treatment of hFP-HEK cells caused a significant delay in G2/M, such that by 9 h, none of these cells had exited mitosis. Even after 15 and 18 h, the G2/M population of $PGF_{2\alpha}$-treated hFP-HEK cells was minimally depleted compared with vehicle-treated hFP-HEK cells. Taken together, these data indicate that $PGF_{2\alpha}$ treatment does not cause a complete cell cycle arrest, rather, it delays G2/M phase progression in hFP-HEK cells.

$PGF_{2\alpha}$ delays mitosis in hFP-HEK cells. The progression through G2 and M phases is orchestrated by the sequential activation and inactivation of the Cdc2/cyclin B1 complex. To ensure the inheritance of complete and accurate copies of the genome there is a G2/M checkpoint that monitors the presence of DNA damage. If damage is detected, the G2/M checkpoint will inhibit the activation of the Cdc2/cyclin B1 complex, thereby preventing entry into mitosis until the damage has been repaired [23]. To further delineate the observed delay in the G2/M phase in hFP-HEK cells treated with $PGF_{2\alpha}$, cyclin B1 expression and Cdc2 kinase activity were assessed by immunoblot analysis and *in vitro* kinase assay, respectively. Surprisingly, as shown

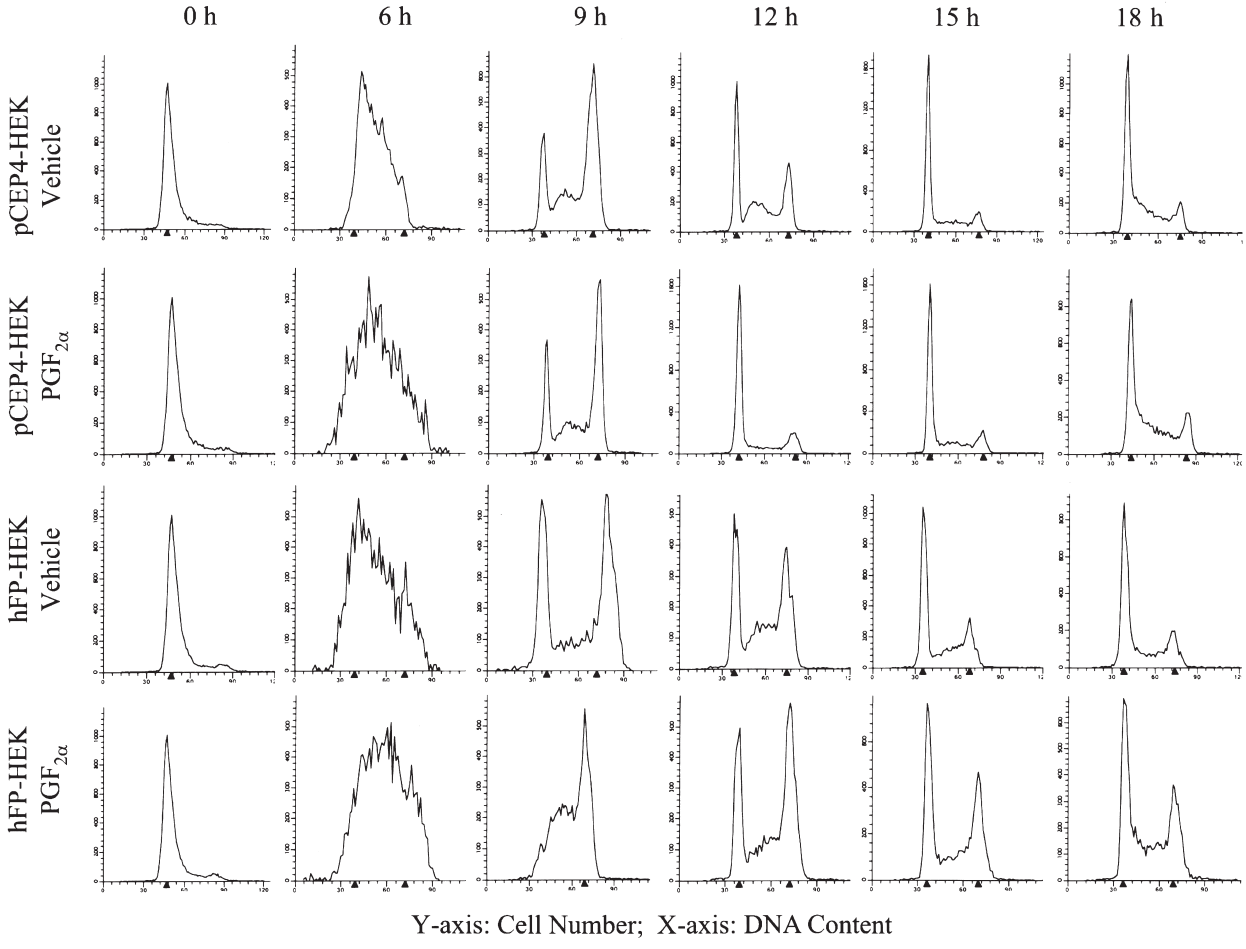

Figure 2. $PGF_{2\alpha}$ causes G2/M delay in HEK cells expressing the human FP prostanoid receptor. DNA profiles of hFP-HEK and pCEP4-HEK cells synchronized in late G1 with the double thymidine-mimosine block. Samples were fixed and stained with propidium iodine at the time of release (0 h), 6 h after release, and then every 3 h up to 18 h after release. For all graphs, the y-axis is cell number and the x-axis is DNA content. Representative of four independent experiments.

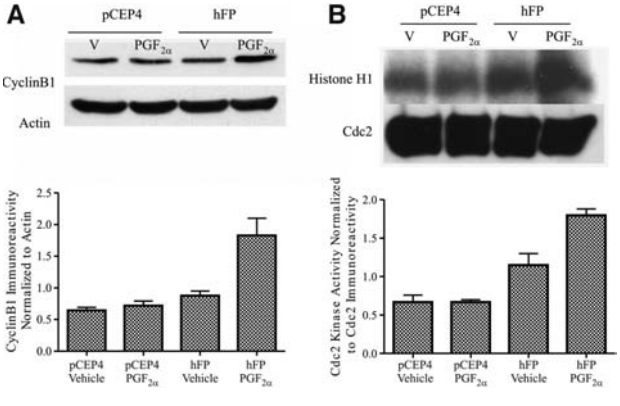

Figure 3. $PGF_{2\alpha}$ treatment of HEK cells stably expressing the human FP prostanoid receptor increases expression of cyclin B1 (*A*) and increases Cdc2-mediated phosphorylation of histone H1 (*B*). (*A*) Upper panel: immunoblot of lysates prepared from hFP-HEK and pCEP4-HEK cells that had been treated with either vehicle (V) or 1 µM $PGF_{2\alpha}$ for 24 h. Blots were probed with anti-cyclin B1 and anti-actin antibodies as described in Materials and methods. Lower panel: quantitative analysis of three independent experiments by densitometry of cyclin B1 immunoreactivity normalized to actin immunoreactivity (means ± SEs). (*B*) Upper panel: autoradiograph of Cdc2 kinase activity (phosphorylation of histone H1) and immunoblot of Cdc2 kinase expression in lysates prepared from hFP-HEK and pCEP4-HEK cells that had been treated with either vehicle (V) or 1 µM $PGF_{2\alpha}$ for 24 h. Cdc2 kinase assays and Cdc2 immunoblotting were done as described in Materials and methods. Lower panel: quantitative analysis of three independent experiments by densitometry of Cdc2 kinase activity (histone H1 phosphorylation) normalized to Cdc2 immunoreactivity (means ± SEs).

in figure 3A, cyclin B1 protein expression was found to increase following treatment of hFP-HEK cells with $PGF_{2\alpha}$. These data indicate that the delay in G2/M was not due to a decrease in cyclin B1 protein expression. As shown in figure 3B, there was a corresponding increase in Cdc2 kinase activity following the treatment of hFP-HEK cells with $PGF_{2\alpha}$, which was not observed in $PGF_{2\alpha}$-treated control pCEP4-HEK cells. These findings indicate that the actions of $PGF_{2\alpha}$ to cause a G2/M delay in hFP-HEK cells are likely to occur following entry into mitosis.

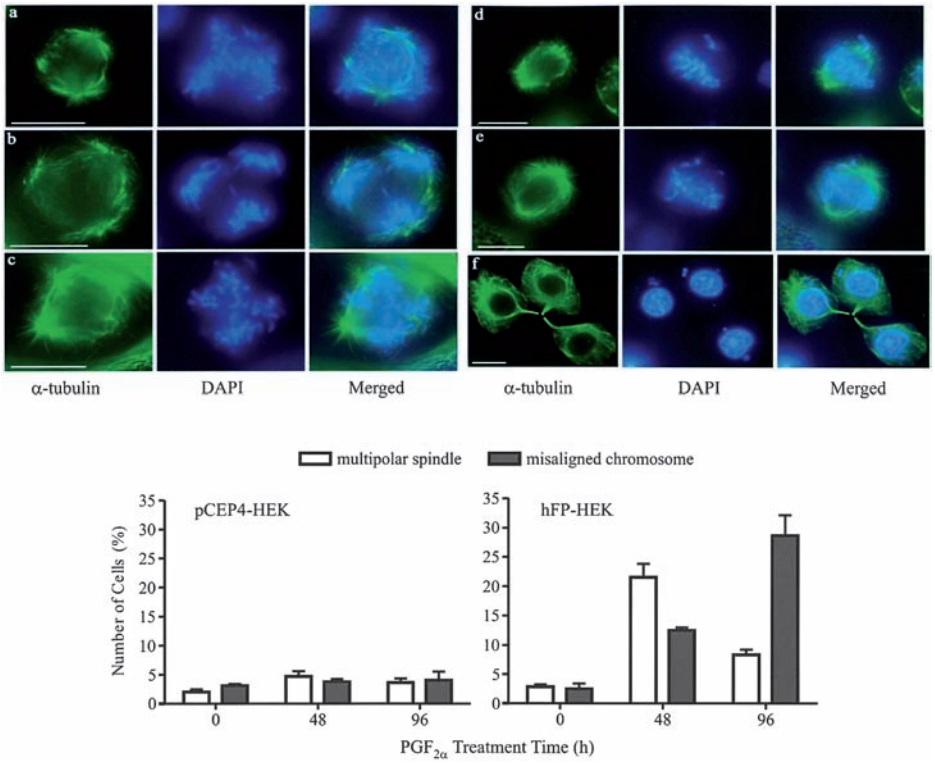

Figure 4. $PGF_{2\alpha}$ induces multipolar mitotic spindles and misaligned chromosomes in HEK cells stably expressing the human FP prostanoid receptor. Upper panels: photomicrographs of hFP-HEK cells after 48 h treatment with 1 μM $PGF_{2\alpha}$ followed by fluorescence labeling of mitotic spindles with anti-α-tubulin antibody (green) and of nuclear DNA with DAPI (blue). a–c, examples of multipolar spindles; d, e, examples of misaligned chromosomes; f, midbody from three polar divisions. Scale bar, 10 μm. Lower panels: the relative percentages of multipolar spindles and misaligned chromosomes in mitotic cells stably transfected with empty vector (pCEP4-HEK) or the human FP prostanoid receptor (hFP-HEK) after treatment with 1 μM $PGF_{2\alpha}$ for 0, 48 or 96 h. Data are the means ± SEs from three independent experiments.

$PGF_{2\alpha}$ treatment leads to the generation of multipolar mitotic spindles and misaligned chromosomes in hFP-HEK cells. Like the G2/M checkpoint, there is a mitotic spindle assembly checkpoint which functions to prevent cells with misaligned chromosomes from exiting mitosis prematurely. Failure of this checkpoint can result in aneuploidy in the daughter cells and contributes to genomic instability. So far, all known delays in mitosis are mediated by the mitotic spindle assembly checkpoint [24]. Because $PGF_{2\alpha}$ delayed mitosis in hFP-HEK cells, we were interested in further assessing the integrity of mitotic spindles and examining the chromosome alignment in hFP-HEK cells following treatment with $PGF_{2\alpha}$. The results of these studies are shown in figures 4 and 5. In contrast to pCEP4-HEK control cells and vehicle-treated hFP-HEK cells, which showed essentially normal bipolar spindle and chromosome alignment, $PGF_{2\alpha}$-treated hFP-HEK cells exhibited a significant portion of cells with multipolar spindles (fig. 4, panels a–c) and misaligned chromosomes (fig. 4, panels d–f). These multipolar spindles were often accompanied by poles of different sizes and with disorganized arrays of microtubules and misaligned chromosomes. The bottom panel of figure 4 shows that the percentage of hFP-HEK cells with multipolar spindles increased ~6-fold 48 h after addition of $PGF_{2\alpha}$, and then decreased at 96 h, but was still ~2.5-fold higher than in the untreated cells. The percentage of hFP-HEK cells with misaligned chromosomes, however, increased markedly both 48 h and 96 h after the addition of $PGF_{2\alpha}$ (~3.5- and 8-fold, respectively). The outcome of these multipolar spindles and misaligned chromosomes is that free and/or lagging chromosomes will distribute randomly to the daughter cells giving rise to either a gain or loss of chromosomes (aneuploidy). Figure 5, in fact, shows that in hFP-HEK cells treated with $PGF_{2\alpha}$ there was a dramatic increase in the percentage of hFP-HEK cells containing micronuclei around the major interphase nuclei, which is a reflection of aneuploidy. Thus, the percentage of hFP-HEK cells containing micronuclei increased from ~2% at the zero time point to ~44% after 96 h of treatment with $PGF_{2\alpha}$. There was also an increase in hFP-HEK cells containing two or more nuclei (polyploidy) following $PGF_{2\alpha}$ treatment; from ~1% at the zero time point to ~10% after 96 h of treatment.

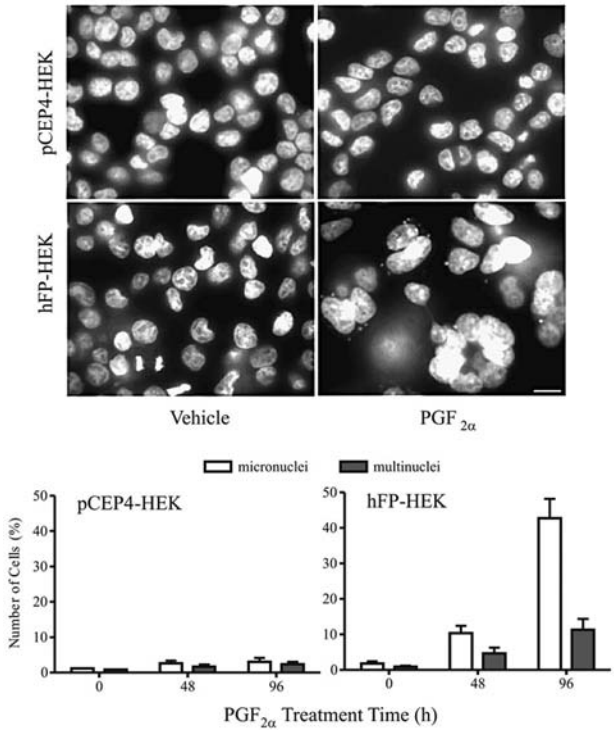

Figure 5. $PGF_{2\alpha}$ induces genomic instability in HEK cells stably expressing the human FP prostanoid receptor. Upper panel: photomicrographs of HEK cells stably transfected with empty vector (pCEP4-HEK) or the human FP prostanoid receptor (hFP-HEK) following 96 h treatment with either vehicle (2% Na_2CO_3) or 1 µM $PGF_{2\alpha}$ and fluorescence labeling of nuclear DNA with DAPI. Scale bar, 10 µm. Lower panel; histograms of the numbers of cells with micronulei or multiple nuclei following 0, 48 or 96 h treatment with 1 µM $PGF_{2\alpha}$. Data are the means ± SEs from five independent experiments. Nuclei with free chromosomes, lagging chromosomes, abnormal shapes and fragmented nuclei were counted as micronuclei (aneuploidy). Cells with two or more nuclei were counted as multinuclei (polyploidy).

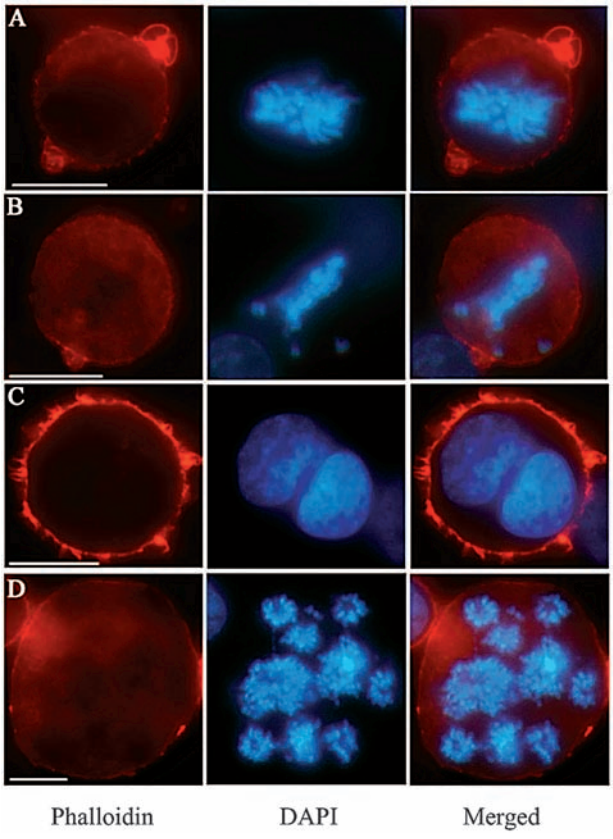

Figure 6. $PGF_{2\alpha}$ induces abnormal cortical activity and generation of multiple nuclei in HEK cells stably expressing the human prostanoid receptor. Photomicrographs of hFP-HEK cells after 96 h treatment with 1 µM $PGF_{2\alpha}$ followed by fluorescence labeling of cortical actin with Texas Red-conjugated phalloidin (red) and of nuclear DNA with DAPI (blue). Scale bar, 10 µm. (*A, B*) Examples of abnormal blebs. (*C*) Example of abnormal mitotic actin staining in a cell with two interphase nuclei. (*D*) Example of multinucleated cell undergoing mitosis.

$PGF_{2\alpha}$ treatment induces abnormal cortical activity during cytokinesis. The presence of polyploidy in $PGF_{2\alpha}$-treated hFP-HEK cells suggests abnormalities during cytokinesis (cell division) as well as during mitosis. This would not be unexpected given that mitosis and cytokinesis are related events requiring close temporal and spatial coordination. Phalloidin staining of actin and fluorescence microscopy were, therefore, used to determine if the presence of multipolar spindles and misaligned chromosomes was associated with any abnormalities in cytokinesis in hFP-HEK cells treated with $PGF_{2\alpha}$. We found that while control pCEP4-HEK and vehicle-treated hFP-HEK cells showed essentially normal patterns of actin staining, $PGF_{2\alpha}$-treated hFP-HEK cells showed numerous instances of abnormal staining. Figure 6 shows several examples of this abnormal staining. Thus, the $PGF_{2\alpha}$ treated hFP-HEK cells shown in panels figure 6A and B showed the presence of abnormal cortical blebs in cells undergoing cytokinesis. Figure 6C shows the presence of a $PGF_{2\alpha}$-treated hFP-HEK cell containing multiple interphase nuclei within a spherical cortex of actin staining, which can result from a failure of cytokinesis. Figure 6D shows the consequence of this abnormal cytokinesis, which is a multi-nucleated cell undergoing mitosis. Numerous examples of multinucleated hFP-HEK cells following $PGF_{2\alpha}$ treatment are shown in figure 5 at lower magnification.

Expression of N19Rho attenuates the cell cycle changes and rescues aneuploidy following treatment of hFP-HEK cells with $PGF_{2\alpha}$. We have previously reported that $PGF_{2\alpha}$ can activate Rho-mediated signaling in HEK cells stably expressing the ovine FP_A and FP_B receptors and that this Rho signaling leads to the activation of focal adhesion kinase and the formation of actin stress fibers [15]. The upper panel of figure 7 shows that $PGF_{2\alpha}$ can also induce the formation of actin stress fibers in HEK cells stably expressing the human FP receptor, but not in

the control cells stably transfected with the pCEP4 vector alone. The Rho inhibitor, C3 exoenzyme and the ROCK inhibitor, Y27632, blocked the $PGF_{2\alpha}$-mediated formation of actin stress fibers in hFP-HEK cells (data not shown). We hypothesized that $PGF_{2\alpha}$-induced Rho signaling might underlie the mechanism of defective cortical activity and failure of cytokinesis.

For these experiments N19RhoA, the dominant negative form of RhoA, was co-transfected with EGFP into hFP-HEK cells. EGFP was used to select the positive cells and cell cycle analysis and quantitation of cells containing micronuclei/multinuclei were carried out 24 and 48 h after $PGF_{2\alpha}$ treatment, respectively. A 96-h time point could not be examined because with the time required for the transfection itself, the cells were postconfluent and were growing in layers by 96-h. As shown in the middle panel of figure 7, treatment of hFP-HEK cells with $PGF_{2\alpha}$ resulted in a twofold increase in the number of cells in G2/M which increased from 12% to 22%. Concomitantly, the number of cells in G0/G1 decreased by roughly the same amount from 43% to 32%, while the S phase population remained unchanged. Transfection with dominant negative N19RhoA alone caused a slight increase in the number of cells in G0/G1, from 43% to 48%, while causing slight decreases of a similar magnitude in the number of cells in S and G2/M. The effects of N19RhoA in the absence of $PGF_{2\alpha}$ treatment suggest a slowing of the cell cycle, which is consistent with the well-known function of Rho in the progression from G1 to S. Rho signaling, however, also appears to be important with respect to the changes in cell cycle distribution that are mediated by $PGF_{2\alpha}$ in hFP-HEK cells. Thus, the middle panel of figure 7 shows that in hFP-HEK cells transfected with N19RhoA, the effect of $PGF_{2\alpha}$ to increase the number of cells in G2/M was essentially blocked. The effect of $PGF_{2\alpha}$ to decrease the number of cells in G0/G1, however, was only slightly reduced in hFP-HEK cells transfected with N19RhoA. These effects were accompanied by a moderate increase in the number of cells in S phase. In contrast, the lower panel of figure 7 shows that the effect of $PGF_{2\alpha}$ to increase the number of hFP-HEK cells with micronuclei following treatment with $PGF_{2\alpha}$ was almost completely abrogated in N19RhoA-transfected hFP-HEK cells, going from about threefold to almost nothing. The effect of $PGF_{2\alpha}$ to increase the number of hFP-HEK cells with multiple nuclei could not be observed in N19RhoA-transfected hFP-HEK cells because the blockade of Rho signaling itself caused a large increase in the number of cells with multiple nuclei even in the absence of $PGF_{2\alpha}$ treatment. Taken together these findings suggest that the observed cell cycle delay and aneuploidy generated by $PGF_{2\alpha}$ treatment of hFP-HEK cells is mediated at least in part by a Rho signaling pathway.

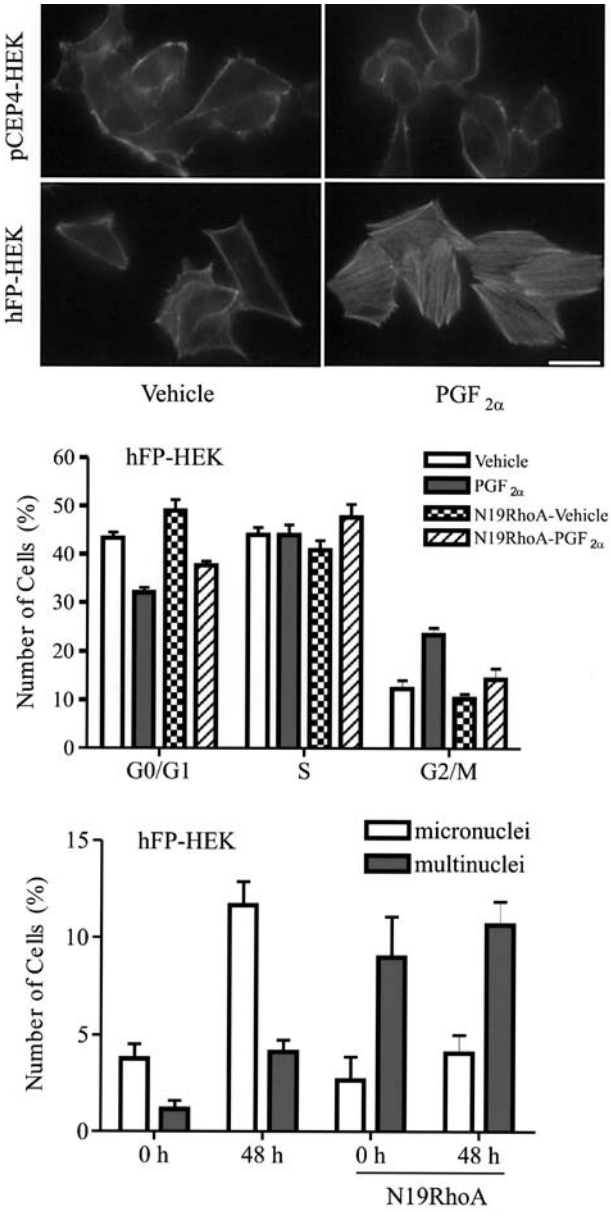

Figure 7. Dominant negative N19RhoA attenuates the cell cycle delay and rescues aneuploidy caused by $PGF_{2\alpha}$ treatment of HEK cells stably expressing the human FP prostanoid receptor. Upper panel: photomicrographs of HEK cells stably transfected with empty vector (pCEP4-HEK) or the human FP prostanoid receptor (hFP-HEK) following 1 h treatment with either vehicle (2% Na_2CO_3) or 1 µM $PGF_{2\alpha}$ and fluorescence labeling of actin stress fibers with Texas Red-conjugated phalloidin. Scale bar, 10 µm. Middle panel: cell cycle distribution of hFP-HEK cells transiently transfected with EGFP alone or EGFP plus N19RhoA, followed by treatment with either vehicle or 1 µM $PGF_{2\alpha}$ for 24 h. Data are the means ± standard errors from four independent experiments. Lower panel: number of cells with micronuclei or multiple nuclei that were transiently transfected with either control plasmid or plasmid encoding N19RhoA and 24 h later were treated with 1 µM $PGF_{2\alpha}$ for 48 h. Data are the means ± SEs from five independent experiments. Cells were stained with DAPI to label nuclear DNA and then examined and quantified by fluorescence microscopy. Micronuclei and multiple nuclei were defined as in the legend to figure 5.

Discussion

The present study was aimed at exploring the possible role of $PGF_{2\alpha}$ signaling in the cell cycle by utilizing a HEK cell line stably expressing the human FP prostanoid receptor. Here we report that $PGF_{2\alpha}$ treatment of hFP-HEK cells leads to a delay in mitosis progression with elevated levels of cyclin B1 and increased Cdc2 kinase activity. In addition, $PGF_{2\alpha}$ treatment of hFP-HEK cells was found to generate abnormal mitotic spindles and misaligned chromosomes resulting in the accumulation of multiple nuclei and aneuploidy. These findings are reminiscent of the outcomes of dysregulation of the centrosomal proteins involved in kinetochore-microtubule attachment [25, 26]. Given that all known delays in mitosis are due to the activation of the mitotic spindle assembly checkpoint, we postulate that the generation of abnormal mitotic spindles and misaligned chromosomes caused by the treatment of hFP-HEK cells with $PGF_{2\alpha}$ activates the mitotic spindle checkpoint and delays the onset of anaphase. Thus, if hFP-HEK cells fail to correct the abnormalities in chromosome alignment during a prolonged mitosis, they are likely to exit mitosis with the generation of one or more cells with altered genomes.

The observation of multinucleated cells after the treatment of hFP-HEK cells with $PGF_{2\alpha}$ further supports the notion that imbalanced Rho GTPase activity results in defective actomyosin contractility and failure of cytokinesis. It is well known that Rho signaling is involved in the progression of G1/S transition and in cytokinesis [27, 28]. Misaligned chromosomes and aneuploidy induced by $PGF_{2\alpha}$ treatment of hFP-HEK cells suggests a potential function of Rho in nuclear division as well. In support of this, ROCK kinase, one of the downstream effectors of Rho, has been found to exist in the same complex with Aurora A kinase. Furthermore, depletion of either protein by RNA interference (RNAi) induces G2/M cell cycle arrest and abnormal mitotic spindles, with the corresponding generation of aneuploidy and polyploidy [29]. Given that Aurora A kinase plays an essential role in centrosome maturation and bipolar spindle assembly, and the evidence that both Aurora A kinase and ROCK exist in the same genetic pathway, lend additional support to the idea that ROCK and its activator, Rho, are involved in the normal functions of the centrosome, spindle assembly, and equal partitioning of the chromosomes. Cdc42 and its effector, mDia3, were recently found to be involved in the bi-orientation and stabilization of spindle microtubule attachment to the kinetochore, which thereby regulates chromosome alignment in metaphase [30]. A possible mechanism that could link $PGF_{2\alpha}$ activation of Rho signaling with the role of Cdc42 in chromosome alignment involves the protein, ECT2, which is a guanine nucleotide exchange factor for the Rho, Rac, and Cdc42 GTPases. Thus, inappropriate activation of Rho in $PGF_{2\alpha}$-treated hFP-HEK cells could interfere with the bi-attachment of the kinetochore to microtubules by depleting ECT2 activity toward Cdc42. Evidence supporting this mechanism is that expression of dominant negative forms of ECT2, and RNAi knockdown of ECT2 protein, impair microtubule attachment to kinetochores and cause prometaphase delay and abnormal chromosomal segregation [31].

Genomic instability involving the gain or loss of chromosomes (aneuploidy) is a hallmark of cancer. One of the important features of cancer-associated aneuploidy is that it appears to be a very dynamic process. Studies suggest that pre-existing aneuploidy in transformed cells is usually associated with elevated rates of subsequent chromosome instability [32]. As reviewed in the Introduction, $PGF_{2\alpha}$ has been found to act as a tumor promoter in a mouse model of skin carcinogenesis. A possible basis for this tumor-promoting activity might, therefore, involve a $PGF_{2\alpha}$-mediated increase in genomic instability caused by interference with proper functioning of the mitotic spindle and equal partitioning of the chromosomes. If true, this would suggest that $PGF_{2\alpha}$ could exert a tumor-promoting action in the very early stages of carcinogenesis.

Support for a tumor-promoting action of prostanoids in general comes from the well-known protective effects of non-steroidal anti-inflammatory drugs on the development of a number of cancers, including colon, breast, and oral cancer [2, 3]. It is interesting that the tissue concentrations of both PGE_2 and $PGF_{2\alpha}$ are frequently highly elevated in inflammation and cancer [1]. Also intriguing is that epithelial cells from high-grade inflammatory bronchi, for example, show a degree of aneuploidy that is similar to that observed in tumor cells. Likewise, centrosome amplification and multipolar mitosis have been found to occur in the early stages of inflammation and are characteristic of tumors as well [33]. Thus, inflammatory conditions share several tumor-specific features that are likely to be maintained by the combined actions of PGE_2, $PGF_{2\alpha}$ and possibly other prostanoids. This study has shown that $PGF_{2\alpha}$ can induce multipolar mitosis and increase aneuploidy in cells transfected with the human FP receptor. Further work will be needed to see if the actions of $PGF_{2\alpha}$ acting through FP receptors are responsible for some of the genomic instability observed in tumors, and whether FP receptor activation is directly involved with early stages of tumorigenesis.

Acknowledgements. The authors thank the Arizona Cancer Center Cytometry Core Facility (Cancer Center Support Grant P30CA23074) for their help with flow cytometric analysis. This work was supported by the National Institutes of Health (grant EY11291) and Allergan Inc.

1 Dubois R. N., Abramson S. B., Crofford L., Gupta R. A., Simon L. S., Van De Putte L. B. et al. (1998) Cyclooxygenase in biology and disease. FASEB J. **12:** 1063–1073
2 Lupulescu A. (1996) Prostaglandins, their inhibitors and cancer. Prostaglandins Leukot. Essent. Fatty Acids **54:** 83–94
3 Zha S., Yegnasubramanian V., Nelson W. G., Isaacs W. B. and De Marzo A. M. (2004) Cyclooxygenases in cancer: progress and perspective. Cancer Lett. **215:** 1–20
4 Liu C. H., Chang S. H., Narko K., Trifan O. C., Wu M. T., Smith E. et al. (2001) Overexpression of cyclooxygenase-2 is sufficient to induce tumorigenesis in transgenic mice. J. Biol. Chem. **276:** 18563–18569
5 Neufang G., Furstenberger G., Heidt M., Marks F. and Muller-Decker K. (2001) Abnormal differentiation of epidermis in transgenic mice constitutively expressing cyclooxygenase-2 in skin. Proc. Natl. Acad. Sci. USA **98:** 7629–7634
6 Sheng H., Shao J., Morrow J. D., Beauchamp R. D. and DuBois R. N. (1998) Modulation of apoptosis and Bcl-2 expression by prostaglandin E2 in human colon cancer cells. Cancer Res. **58:** 362–366
7 Sheng H., Shao J., Washington M. K. and DuBois R. N. (2001) Prostaglandin E2 increases growth and motility of colorectal carcinoma cells. J. Biol. Chem. **276:** 18075–18081
8 Miyauchi-Hashimoto H., Kuwamoto K., Urade Y., Tanaka K. and Horio T. (2001) Carcinogen-induced inflammation and immunosuppression are enhanced in xeroderma pigmentosum group A model mice associated with hyperproduction of prostaglandin E2. J. Immunol. **66:** 5782–5791
9 Fujino H. and Regan J. W. (2003) Prostanoid receptors and phosphatidylinositol 3-kinase: a pathway to cancer? Trends Pharmacol. Sci. **24:** 335–340
10 Abramovitz M., Boie Y., Nguyen T., Rushmore T. H., Bayne M. A., Metters K. M. et al. (1994) Cloning and expression of a cDNA for the human prostanoid FP receptor. J. Biol. Chem. **269:** 2632–2636
11 Ito S., Sakamoto K., Mochizuki-oda N., Ezashi T., Miwa K., Okuda-Ashitaka E. et al. (1994) prostaglandin F2 alpha receptor is coupled to Gq in cDNA-transfected Chinese hamster ovary cells. Biochem. Biophys. Res. Commun. **200:** 756–762
12 Hekeda Y., Shiokawa M., Mano H., Kameda T., Raisz L. G. and Kumegawa M. (1997) Prostaglandin F2alpha stimulates tyrosine phosphorylation and mitogen-activated protein kinase in osteoblastic MC3T3-E1 cells via protein kinase C activition. Endocrinology **138:** 1821–1828
13 Chen D. B., Westfall S. D., Fong H. W., Roberson M. S. and Davis J. S. (1998) Prostaglandin F2alpha stimulates the Raf/MEK1/mitogen-activated protein kinase signaling cascade in bovine luteal cells. Endocrinology **139:** 1876–1885
14 Melien O., Thoresen G. H., Sandnes D., Ostby E. and Christoffersen T. (1998) Activation of p42/p44 mitogen-activated protein kinase by angiotensin II, vasopressin, norepinephrine, and prostaglandin F2alpha in hepatocytes is sustained, and like the effect of epidermal growth factor, mediated through pertussis toxin-sensitive mechanisms. J. Cell. Physiol. **175:** 348–358
15 Pierce K. L., Fujino H., Srinivasan D. and Regan J. W. (1999) Activation of FP prostanoid receptor isoforms leads to Rho-mediated changes in cell morphology and in the cell cytoskeleton. J. Biol. Chem. **274:** 35944–35949
16 Nurse P. (1997) Regulation of the eukaryotic cell cycle. Eur. J. Cancer **33:** 1002–1004
17 Doree M. (1990) Control of M-phase by maturation-promoting factor. Curr. Opin. Cell Biol. **2:** 269–273
18 Furstenberger G., Gross M. and Marks F. (1989) Eicosanoids and multistage carcinogenesis in NMRI mouse skin: role of prostaglandin E and F in conversion (first stage of tumor promotion) and promotion (second stage of tumor promotion). Carcinogenesis **10:** 91–96
19 Wolfle D. (2003) Enhancement of carcinogen-induced malignant cell transformation by prostaglandin $F_{2\alpha}$. Toxicology **188:** 139–147
20 Weber T. J., Markillie L. M., Chrisler W. B., Vielhauer G. A. and Regan J. W. (2002) Modulation of JB6 mouse epidermal cell transformation response by the prostaglandin F2alpha receptor. Mol. Carcinog. **35:** 163–172
21 Sales K. J., Milne S. A., Williams A. R. anderson R. A. and Jabbour H. N. (2004) Expression, localization, and signaling of prostaglandin F2 alpha receptor in human endometrial adenocarcinoma: regulation of proliferation by activation of the epidermal growth factor receptor and mitogen-activated protein kinase signaling pathways. J. Clin. Endocrinol. Metab. **89:** 986–993
22 Matsushime H., Quelle D. E., Shurtleff S. A., Shibuya M., Sherr C. J. and Kato J. Y. (1994) D-type cyclin-dependent kinase activity in mammalian cells. Mol. Cell Biol. **14:** 2066–2076
23 Smits V. A. and Medema R. H. (2001) Checking out the G (2)/M transition. Biochem. Biophys. Acta **1519:** 1–12
24 Riedar C. L. and Maiato H. (2004) Stuck in division or passing through: what happens when cells cannot satisfy the spindle assemble checkpoint. Dev. Cell **7:** 637–651
25 Zhou H., Kuang J., Zhong L., Kuo W. L., Gray J. W., Sahin A. et al. (1998) Tumour amplified kinase STK15/BTAK induces centrosome amplification, aneuploidy and transformation. Nat. Genet. **20:** 189–193
26 Sumara I., Giménez-Abián J. F., Gerlich D., Hirota T., Kraft C., Torre C. et al. (2004) Roles of Polo-like kinase 1 in the assembly of functional mitotic spindles. Curr. Biol. **14:** 1712–1722
27 Olson M. F., Ashworth A. and Hall A. (1995) An essential role of Rho, Rac, and Cdc42 GTPases in cell cycle progression through G1. Science **269:** 1270–1272
28 Kimura K., Tsuji T., Takada Y., Miki T. and Narumiya S. (2000) Accumulation of GTP-bound rhoA during cytokinesis and a critical role of ECT2 in this accumulation. J. Biol. Chem. **275:** 17233–17236
29 Du J. and Hannon G. J. (2004) Suppression of p160ROCK bypasses cell cycle arrest after Aurora-A/STK15 depletion. Proc. Natl. Acad. Sci. USA **101:** 8975–8980
30 Yasuda S., Oceguera-Yanez F., Kato T., Okamoto M., Yonemura S., Terada Y. et al. (2004) Cdc42 and mDia3 regulate microtubule attachment to kinetochores. Nature **428:** 767–771
31 Oceguera-Yanez F., Kimura K., Yasuda S., Higashida C., Kitamura T., Hiraoka Y. et al. (2005) Ect2 and MgcRacGAP regulate the activation and function of Cdc42 in mitosis. J. Cell Biol. **168:** 221–232
32 Duesberg P., Rausch C., Rasnick D. and Hehlmann R. (1998) Genetic instability of cancer cells is proportional to their degree of aneuploidy. Proc. Natl. Acad. Sci. USA **95:** 13692–13697
33 Lothschutz D., Jennewein M., Pahl S., Lausberg H. F., Eichler A., Mutschler W. et al. (2002) Polypoloidization and centrosome hyperamplification in inflammatory bronchi. Inflamm. Res. **51:** 416–422

To access this journal online:
http://www.birkhauser.ch